Large Circular Dichroism Ellipticities for N-Templated Helical Polypeptides Are Inconsistent with Currently Accepted Helicity Algorithms**

Peter Wallimann, Robert J. Kennedy, and Daniel S. Kemp*

Among polypeptide conformations, only helices permit calculation of conformational stability from a readily measurable physical parameter. If a polypeptide exhibits a helical circular dichroism (CD) spectrum (intense positive maximum near 190 nm, negative minima at 208 and 222 nm), Equation (1) is generally used to relate the average fractional helicity[1] (FH) to the experimental mean residue molar ellipticity[2a,c] ($[\theta]_{222}$). The limiting ellipticity $[\theta_{H\infty}]_{222}$ of Equation (1) corresponds to a completely helical peptide of infinite length, and the term $(1-x/N$; where $N=$ peptide length; $2.4<x<4.5)$ provides a finite length correction.[3] From studies of N-templated peptides containing more than twelve amino acid residues, we now demonstrate that literature values underestimate both $[\theta_{H\infty}]_{222}$ and its length dependence.

$$FH=\frac{[\theta]_{222}}{[\theta_{H\infty}]_{222}\left(1-\frac{x}{N}\right)} \quad (1)$$

$$[\theta_H]_{222}=(-44000+250\,T)\left(1-\frac{2.5}{N}\right)=100\,\%\text{ helicity for length }N \quad (2)$$

Certain alanine-rich peptides containing lysine or arginine are reported to approach FH values of 0.7 to 0.8 in water at low temperature,[2b] but no peptide has been unequivocally proven to be 100 % helical. Cited $-[\theta_{H\infty}]_{222}$ values of 37 000 to 44 000 deg cm^2 dmol^{-1} are usually extrapolated as limits of a series of temperature- or additive-dependent CD spectra.[2c, 4]

Ellipticities of peptides that are amide-linked to an efficient helix initiator such as the N-terminal cap AcHel[5] should give a better approximation to $[\theta_{H\infty}]_{222}$. Figure 1 shows helical CD spectra at 5 °C intervals for the N-templated 22-residue peptide **1**, AcHel-$(Ala_4Lys)_4Ala_2$-NH_2, in water containing 16 mol % of ethylene glycol, which permits CD measurements at sub-zero temperatures. The value of $-[\theta]_{222}$ increases dramatically as the temperature is lowered, but does not converge to a limit. At the frequently studied temperature of 2 °C, $-[\theta]_{222}$ for **1** is 50 900 deg cm^2 dmol^{-1}, corresponding to 1.32 times the largest reported temperature- and length-corrected value of $[\theta_H]_{222}$ [Eq. (2)].[4b,c] Similar values and temperature dependencies for $-[\theta]_{222}$ of **1** were observed at

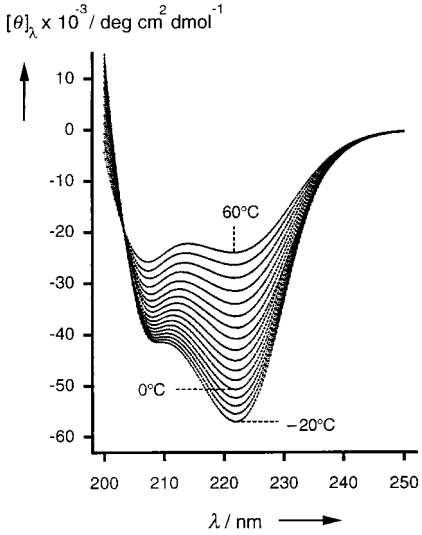

Figure 1. Overlay of 17 CD spectra of AcHel-$(Ala_4Lys)_4Ala_2$-NH_2 measured in 5 °C intervals between −20 and 60 °C in 16 mol % ethylene glycol in water (pH 1, 0.2 mol L^{-1} $NaClO_4$). Peptide concentration: 45 μmol L^{-1}.

pH 1 in aqueous NaCl (5 mol L^{-1}) and in aqueous 2,2,2-trifluoroethanol at pH < 2.

Are the low temperature CD properties of **1** unique? Figure 2 depicts values of $-[\theta]_{222}$ measured in water at 2 °C for N-templated peptides AcHel-$(Ala_4Lys)_nAla_2$-NH_2, $n=1$

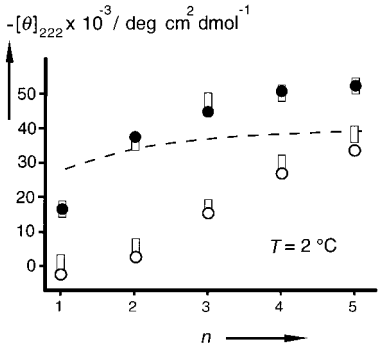

Figure 2. Effect of oligomer length n on the $-[\theta]_{222}$ value for N-templated AcHel-$(Ala_4Lys)_nAla_2$-NH_2 (filled circles) and N-protonated $H_2^+(Ala_4Lys)_nAla_2$-NH_2 (open circles) (2 °C, pH 1, 0.2 mol L^{-1} $NaClO_4$). The dashed line shows the calculated length dependence for $[\theta_H]_{222}$ from Equation (2). For the templated series, $n>1$, the experimental values exceed this predicted limit. The open rectangles give $[\theta]_{222}$ values calculated from Equation (3), as described in the text and supporting information. Experimental $[\theta]_{222}$ values are corrected for the contribution of AcHel (less than 1 % for $n>2$).

to 5, and for the analogous N-protonated peptides $H_2^+(Ala_4Lys)_nAla_2$-NH_2. Data are also available for the series AcHel-$(Ala_4Lys)_3Ala_n$-NH_2, $n=0$ to 6, and for the conjugates AcHel-$Ala_4Glu(Ala_4Lys)_2Ala_2$-$NH_2$ and AcHel-$(Ala_4Lys)_2$-Ala_7-X-NH_2 (X = Lys or Arg). For these ten partially helical AcHel peptides with $16<N<22$, the $-[\theta]_{222}$ values in water at 2 °C pH 1 exceed $-[\theta_H]_{222}$ values for 100 % helical peptides predicted from Equation (2), with a mean ratio, $[\theta]_{222}/[\theta_H]_{222}=1.14$ (± 0.04).

Could the presence of the template significantly bias the CD spectra of the conjugates? The contribution of the

[*] Prof. D. S. Kemp, Dr. P. Wallimann, R. J. Kennedy
Department of Chemistry, Rm. 18–582
Massachusetts Institute of Technology, Cambridge, MA 02139 (USA)
Fax: (+1) 617-258-7500
E-mail: kemp@ucockatoo.mit.edu

[**] This research was supported by the National Institutes of Health (GM 13453), the National Science Foundation (9121702-CHE), and by the Swiss National Science Foundation (fellowship to P.W.). We thank Prof. Klaus Biemann for MALDI MS and Prof. Peter Kim for providing access to the ultracentrifuge.

Supporting information for this article is available on the WWW under http://www.wiley-vch.de/home/angewandte/ or from the author.

  1433-7851/99/3809-1290 $ 17.50+.50/0

template CD chromophore to $-[\theta]_{222}$ of highly helical peptides is small.[5b] More significantly, low temperature CD spectra of nontemplated peptides can be superimposed on corresponding spectra of their AcHel conjugates measured at higher temperatures (Figure 3). Thus the template merely

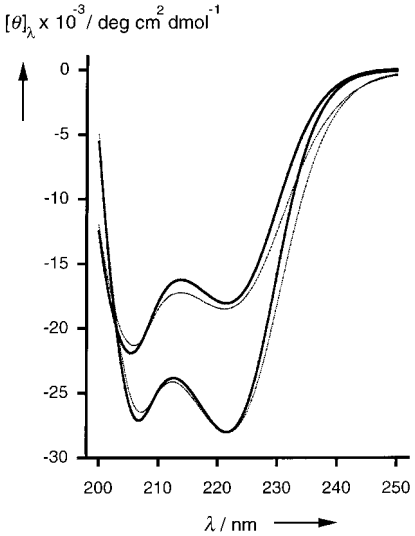

Figure 3. CD curve shape comparisons (pH 1, 0.2 mol L^{-1} $NaClO_4$). Light curves: AcHel-$(Ala_4Lys)_4Ala_2$-NH_2 at 40 °C (lower spectrum) and 55 °C (upper spectrum). Bold curves: $H_2^+(Ala_4Lys)_4Ala_2$-NH_2 at 0 °C (lower spectrum) and 20 °C (upper spectrum).

stabilizes the peptide helix, while preserving all details of its CD spectrum.

Values of $[\theta]_{222}$ for templated and nontemplated pepides of Figure 2 show trends that are consistent with FH values calculated from the Lifson – Roig equation (L – R), which uses the peptide length N, an initiation constant v, and amino acid helical propensities w as variables.[6] A L – R calculation treats a helical peptide as a manifold of nonhelical, completely helical, and partially helical conformations and assigns to each helical conformation a relative abundance, expressed as a mole fraction χ_H. The fractional helicity FH of a single helical conformation is k/N, where k is the length of its helical region, and each conformation thus contributes $\chi_H(k/N)$ to the overall FH. For the short ($n = 1$ or 2) nontemplated peptides studied under the conditions of Figure 2, the most abundant conformations are nonhelical, but for $n = 3$, 4, and 5, the helical conformations dominate. This difference results in a dramatic increase of FH with length, as shown by the sigmoid shape of the $-[\theta]_{222}$ plot. The very different monotonic shape of the plot for the templated peptide series reflects the role of the template as an efficient helix initiator. For all N-templated peptides the helical conformations dominate.

The template also selectively increases the χ_H of conformations with long helical regions. This effect explains a second feature of the data in Figure 2. For $n = 4$ or 5, the templated peptides exhibit much larger $-[\theta]_{222}$ values. Since k/N approaches 1 for these conformations, they contribute maximally to FH and to $-[\theta]_{222}$. By contrast, the helical manifolds for nontemplated peptides are dominated by many conformations containing short helical regions. These have smaller k/N values and contribute inefficiently to FH.

The L – R equation thus models the data of Figure 2 qualitatively. For quantitative modeling, a revised version of Equation (2) is needed. The dotted line of Figure 2 gives values of $-[\theta_H]_{222}$ calculated from Equation (2) that predict the experimental $-[\theta]_{222}$ value expected for a hypothetical peptide with a FH of 1.0. Calculated FH values for the templated peptides with $n = 3$–5 fall in the range of 0.81 to 0.85, and thus Equation (2) grossly underestimates the experimental $-[\theta]_{222}$ values. Dividing $-[\theta]_{222}$ for $n = 5$ by its FH yields 61 000 as an approximate value for $-[\theta_H]_{222}$ in this helical length range ($k > 20$). The corresponding value for the first templated peptide ($n = 1$, $k \leq 7$) is 30 000. Redefined values for $-[\theta_H]_{222}$ must clearly double within the peptide size range of 7 to 20 residues, and improved models for calculating $-[\theta]_{222}$ must assign substantially different $[\theta_H]_{222}$ values to conformations containing large and small helical regions.

A simple two-state model accommodates the data of Figure 2. FH can be written as $FH_{small} + FH_{large}$ and distinct $[\theta_H]_{222}$ values can be assigned to each FH term [Eq. (3)].

$$[\theta_H]_{222\ calculated} = [\theta_H]_{222\ small}FH_{small} + [\theta_H]_{222\ large}FH_{large} \quad (3)$$

We define FH_{small} to include conformations with $k \leq 11$ helical residues and set $[\theta_H]_{222\ small}$ equal to Equation (2), $N = 11$, which provides a good fit for $[\theta]_{222}$ in this size range.[7] We define FH_{large} to include conformations with $k > 11$ and set $[\theta_H]_{222\ large}$ equal to $-61\,000$. Values for the AcHel N-capping template parameter, the initiation parameter, and helical propensities for Ala and Lys have all been reported previously.[2, 5c] As seen in Figure 2, with these parameters, Equation (3) allows an excellent fit to the experimental $[\theta]_{222}$ value for the templated series AcHel-$(Ala_4Lys)_nAla_2$-NH_2. The $[\theta]_{222}$ value for the nontemplated peptides of Figure 2 are also accommodated by Equation (3), provided that the average helical propensity is reduced by 9% to compensate for the helix-destabilizing effect of the N-terminal positive charge. This agreement, achieved for a limited data set using a simple two-state model, represents a first step toward a more rigorous relationship between $[\theta]_{222}$ and FH. A larger data base exploring length dependence will be needed to refine the model.

Is the 222 nm minimum appropriate for correlation of $[\theta]$ with FH? Though universally used, experimentally convenient, and relatively insensitive to the presence of nonhelical conformations, $[\theta]_{222}$ may be less reliable than $[\theta]_{208}$, which is cited in the older literature.[8] The two short wavelength helical CD extrema at 195 nm and 208 nm correspond to perpendicular and parallel π-π* electronic transitions and have been modeled satisfactorily by theory, but the 222 nm n-π* band has not.[9] Moreover, large variations in the ratio of $[\theta]_{208}$ to $[\theta]_{222}$ have been reported for helical peptides and these are evident in the data of Figure 1. Although this ratio has been correlated with the relative proportions of α and 3_{10} helical conformations within the helical manifold, the assignment of the limiting CD spectra for pure α and 3_{10} states remains controversial.[10] It is unclear which $[\theta]$ value provides the better correlation with the overall FH, $FH(\alpha) + FH(3_{10})$.

  1433-7851/99/3809-1291 $ 17.50+.50/0

Within our study two questions remain. The large length dependence of $-[\theta_H]_{222}$ in the range of 7 to 20 residues has been demonstrated by an independent method,[11] but its cause is unknown. The preliminary two-state model outlined above appears to be inconsistent with experimental $[\theta]_{222}$ values reported for peptides with $N > 30$. Experiments to explore these issues are in progress, but their outcomes should not change our most important conclusion. For the class of alanine-rich, lysine-containing peptides with $15 > N > 27$, the literature equations relating FH to experimental $[\theta]_{222}$ values underestimate $[\theta_H]_{222}$,[12] and the corresponding FH values are overestimated by 25–50%.

Experimental Section

Peptides were prepared as previously described[5d] and purified by repeated reverse-phase high-performance liquid chromatography (RP-HPLC), and characterized by MALDI-MS (matrix-assisted laser desorption ionization mass spectrometry) and amino acid analysis. The purity of all compounds is estimated to be higher than 95%. Solutions were maintained at pH 1–2 for consistency with NMR measurements, and $NaClO_4$ buffers were used for consistency with literature measurements. CD spectra were taken on a thermostated Aviv 62DS circular dichroism spectrometer calibrated according to literature procedures.[13] Concentrations of CD solutions were determined within 5% error both by a quantitative ninhydrin assay[7b] and by amino acid analysis.[14] Solutions of AcHel-(Ala$_4$Lys)Ala$_2$-NH$_2$ ($n = 4,5$) and selected nontemplated analogues were shown to be monomeric both by CD dilution studies and analytical ultracentrifugation.

Received: August 25, 1998
Revised version: February 1, 1999 [Z12332IE]
German version: *Angew. Chem.* **1999**, *111*, 1377–1379

Keywords: circular dichroism · helical structures · peptides

[1] FH is the fraction of the interior backbone α-carbon atoms of a peptide that belong to helices. Interior α-carbon atoms are flanked by pairs of amide residues.

[2] a) A. Chakrabartty, T. Kortemme, R. L. Baldwin, *Protein Science* **1994**, *3*, 843–852; b) S. Marqusee, V. H. Robbins, R. L. Baldwin, *Proc. Natl. Acad. Sci.* USA **1989**, *86*, 5286–5290; c) S. Padmanabhan, S. Marqusee, T. Ridgeway, T. M. Laue, R. L. Baldwin, *Nature* **1990**, *344*, 268–270.

[3] P. J. Gans, P. C. Lyu, M. C. Manning, R. W. Woody, N. R. Kallenbach, *Biopolymers* **1991**, *31*, 1605–1614.

[4] a) J. M. Scholtz, D. Barrick, E. J. York, J. M. Stewart, R. L. Baldwin, *Proc. Natl. Acad. Sci. USA* **1995**, *92*, 185–189, and references therein; b) P. Luo, R. L. Baldwin, *Biochemistry* **1997**, *36*, 8413–8421; c) J. M. Scholtz, H. Qian, E. J. York, J. M. Stewart, R. L. Baldwin, *Biopolymers* **1991**, *31*, 1463–1470.

[5] AcHel-OH = (2*S*,5*S*,8*S*,11*S*)-1-Acetyl-1,4-diaza-3-oxo-5-carboxy-10-thiatricyclo[2.8.1.0^{4,8}]tridecane. a) D. S. Kemp, S. L. Oslick, T. J. Allen, *J. Am. Chem. Soc.* **1996**, *118*, 4249–4255; b) D. S. Kemp, T. J. Allen, S. L. Oslick, *J. Am. Chem. Soc.* **1995**, *117*, 6641–6657; c) P. Renold, K.-Y. Tsang, L. S. Shimizu, D. S. Kemp, *J. Am. Chem. Soc.* **1996**, *118*, 12234–12235; d) K. Groebke, P. Renold, K.-Y. Tsang, T. J. Allen, K. F. McClure, D. S. Kemp, *Proc. Natl. Acad. Sci. USA* **1996**, *93*, 4025–4029.

[6] a) S. Lifson, A. Roig, *J. Chem. Phys.* **1961**, *34*, 1963–1974; b) H. Qian, J. A. Schellman, *J. Phys. Chem.* **1992**, *96*, 3987–3994.

[7] a) D. S. Kemp, T. J. Allen, S. L. Oslick, J. G. Boyd, *J. Am. Chem. Soc.* **1996**, *118*, 4240–4248; b) S. L. Oslick, PhD Thesis, Massachusetts Institute of Technology (USA), **1996**. c) For the data set at hand, $10 < N < 12$ gives similar fits.

[8] N. Greenfield, G. D. Fasman, *Biochemistry* **1969**, *8*, 4108–4116.

[9] M. C. Manning, R. W. Woody, *Biopolymers* **1991**, *31*, 569–586.

[10] a) C. Toniolo, A. Polese, F. Formaggio, M. Crisma, J. Kamphuis, *J. Am. Chem. Soc.* **1996**, *118*, 2744–2745; b) N. H. Andersen, Z. Liu, K. S. Prickett, *FEBS Lett.* **1996**, *399*, 47–52; c) T. S. Sudha, E. K. S. Vijayakumar, P. Balaram, *Int. J. Peptide Protein Res.* **1983**, *22*, 464–468.

[11] L. S. Shimizu, PhD Thesis, Massachusetts Institute of Technology (USA), **1997**.

[12] For supporting evidence, see: N. D. Lazo, D. T. Downing, *Biochemistry* **1997**, *36*, 2559–2565.

[13] G. C. Chen, J. T. Yang, *Anal. Lett.* **1977**, *10*, 1195–1207.

[14] Biopolymers Lab, MIT, USA.

$[M_3V_{18}O_{42}(H_2O)_{12}(XO_4)]\cdot 24H_2O$ (M = Fe, Co; X = V, S): Metal Oxide Based Framework Materials Composed of Polyoxovanadate Clusters**

M. Ishaque Khan,* Elizabeth Yohannes, and Robert J. Doedens

The early transition metal oxide clusters with M=O functionalities constitute a fast emerging class of compounds. Their properties are of both intrinsic and applied interest and envelop such diverse fields as analytical chemistry, biochemical and geochemical processes, catalysis, materials science, and medicine.[1] Metal oxide clusters with molecular weights at par with proteins have been prepared and characterized.[1e] The structure and bonding patterns in these molecular aggregates remarkably resemble the complex transition metal oxide surfaces[1a, 2] employed as catalysts for organic transformations.[2d, 3] Many such catalysts are poorly understood because of their inaccessibility to conventional physicochemical techniques and therefore are not amenable to improvements in their performances. With their proven role in catalysis[4] and in the development of new oxide-supported transition metal catalysts,[4f] metal oxide clusters offer attractive building units with well-defined properties[5, 1b] for the preparation of catalysts and novel surfaces based on metal (and mixed-metal) oxides whose performance could possibly be rationalized in terms of their constituents at the molecular level.[4a]

However, the technique of bringing suitable metal oxide building units together to generate true metal oxide surfaces and framework materials without the incorporation of additional conventional ligands is still in its infancy and has been limited to the synthesis of mainly one-dimensional chains.[6] Here, we report the synthesis and characterization of two

[*] Prof. M. I. Khan, E. Yohannes
Department of Biological, Chemical, and Physical Sciences
Illinois Institute of Technology
Chicago, IL 60616 (USA)
Fax: (+1) 312-567-3494
E-mail: chemkhan@charlie.iit.edu
Prof. R. J. Doedens
University of California, Irvine, CA 92697 (USA)

[**] This work was supported by the Illinois Institute of Technology.

  1433-7851/99/3809-1292 $ 17.50+.50/0